 CMES, vol.54, no.2, pp.121-145, 2009

Radiative Properties Estimation with the Luus-Jaakola and the Particle Collision Algorithm

D. C. Knupp[1], A. J. Silva Neto[2] and W. F. Sacco[3]

Abstract: The inverse analysis of radiative transfer in participating media has several practical applications. In most cases, the inverse problem is formulated implicitly and the solution is given by the minimization of an objective function. Gradient based methods have largely been used for that purpose, but it has been observed in recent years an increasing interest in the use of stochastic methods. In this work, it is proposed the use of the Luus-Jaakola method and the Particle Collision Algorithm. The former is a random search optimization method that has been successfully employed mainly in chemical engineering, and the latter is a novel stochastic method inspired by the physics of the interaction of nuclear particles inside nuclear reactors. The solutions obtained with these methods are analyzed and compared for different test cases.

Keywords: Radiative Transfer, Inverse Problems, Luus-Jaakola, Particle Collision Algorithm

1 Introduction

Several methodologies have been developed during the last few decades for the formulation and solution of inverse problems in heat transfer, and has been the subject of intensive research with practical applications in several areas. Just to cite a few recent published papers, Yeih and Liu (2009) used a two-stage Lie-group shooting method (TSLGSM) to tackle an inverse problem formulated as a three-point boundary value problem in order to estimate a time-dependent heat source. Mossi, Vielmo, França and Howell (2008) solved an inverse boundary design problem of

[1] Agencia Nacional de Transportes Terrestres, ANTT, Rio de Janeiro-RJ, Brazil. Graduate Student at Universidade Federal do Rio de Janeiro, UFRJ/COPPE, Rio de Janeiro-RJ, Brazil – e-mail:diego.knupp@antt.gov.br

[2] Department of Mechanical Engineering and Energy, Instituto Politécnico, IPRJ, Universidade do Estado do Rio de Janeiro, Nova Friburgo-RJ, Brazil – e-mail: ajsneto@iprj.uerj.br

[3] Universidade Federal do Oeste do Pará, UFOPA, Santarém-PA, Brazil – e-mail: wf-sacco@iprj.uerj.br

combined radiative and turbulent convective heat transfer using the TSVD regularization method. Weig, Liu and Xiang (2009) used the well-known Gauss-Newton in least-squares estimation for the parameter identification and development of a numerical method to estimate the maximal temperature gradients reached in ?redamaged concrete structures. Sladek, Sladek, Wen and Hon (2009) used the meshless local Petrov-Galerkin method (MLPG) to solve an inverse heat conduction problem of predicting the distribution of the heat transfer coefficient on boundaries. Ranjbar, Ezzati and Famouri (2009) used the conjugate gradient method to estimate the metal-mold interfacial heat transfer coefficient (IHTC) in the solidification of Sn-10% Pb.

The formulation and solution of direct and inverse radiative transfer problems is related with several relevant applications such as atmospheric simulation [Buehler, Eriksson, Kuhn, Engeln and Verdes (2005)], analysis of thermal damage in biological tissues [Zhou, Chen and Zhang (2007)], crystal growth processes [Tsukada, Kobayashi, Jing and Imaishi (2005)], optical tomography [Kim and Charette (2007)], computerized tomography [Carita Montero, Roberty and Silva Neto (2004)], hydrological optics [Chalhoub and Campos Velho (2001)], earth remote sensing [Weng (2009); Toomey, Roberts and Nelson (2009)], solar system bodies research [Hillier (1997); Morishima, Salo and Ohtsuki (2009)] and radiative properties estimation [Nenarokomov and Titov (2005); Hespel, Mainguy and Greffet (2003); An, Ruan and Qi (2007)], among many others.

In the present work we focus on the estimation of the optical thickness, single scattering albedo and diffuse reflectivities of one-dimensional homogeneous participating media. For the direct problem solution it is used the Chandrasekhar's discrete ordinates method [Chandrasekhar (1960)] combined with the finite-difference method. The inverse problem is formulated implicitly [Silva Neto (2002); Silva Neto, Roberty, Pinheiro and Alvarez Acevedo (2007)] and the main focus becomes the minimization of an objective function given by the summation of the squared residues between a calculated and a measured quantity.

For the optimization purpose and consequent solution of inverse radiative transfer problems, in recent years we have used a number of deterministic, stochastic and hybrid (combined) methods with particular emphasis on: (i) Levenberg-Marquardt method (LM); (ii) Simulated Annealing (SA); (iii) Genetic Algorithms (GA); (iv) Artificial Neural Networks (ANN); (v) Ant Colony System (ACS); (vi) Particle Swarm Optimization (PSO); (vii) Generalized Extremal Optimization (GEO); (vii) Interior Points Method (IPM); and (ix) combinations of the previous methods.

Gradient based methods, such as the Levenberg-Marquardt, are usually very fast in their convergence when a suitable initial guess is given, but they may get trapped in the closer local minimum.

Even though stochastic methods are known to be computer-intensive, they have been used to solve many practical problems which cannot be satisfactorily solved using deterministic algorithms. With the progress of the computing machines it has been observed a renewed interest in the use of these methods in recent years.

In this work, for the minimization of the objective function, and consequently the solution of the inverse problem, it is proposed the use of the Luus-Jaakola method (LJ) and the Particle Collision Algorithm (PCA).

The Luus-Jaakola method [Luus and Jaakola (1973)] has been successfully employed mainly in chemical engineering, and recent papers show a favorable comparison of this method against other well established stochastic methods [Liao and Luus (2005); Sacco, Alves Filho and Platt (2008)].

The Particle Collision Algorithm is a novel stochastic optimization method proposed by [Sacco, Oliveira and Pereira (2006)], which is inspired by the physics of the interaction of nuclear particles inside nuclear reactors. The great advantage of PCA with respect to other optimization algorithms such as the genetic algorithm, simulated annealing or particle swarm optimization is that, other than the number of iterations, it does not require any additional parameters.

The PCA can be applied to continuous or discrete optimization problems by just changing the perturbation function, while in genetic algorithms, for example, it is necessary to apply special operators for discrete optimization problems [Goldberg (1989)]. Results from the literature show that the PCA outperforms other metaheuristics with less computational effort [Sacco, Lapa, Pereira e Alves Filho (2008)]. It should be stressed that the PCA is extremely easy to implement.

2 Mathematical formulation and solution of the direct problem

Consider a one-dimensional participating medium, i.e. absorbing, scattering and emitting, with thickness L, whose boundaries reflect diffusely the radiation that comes from the interior of the medium. The boundary surfaces at $x = 0$ and $x = L$ are subjected to the incidence of radiation originated at external sources with intensities F_1 and F_2, respectively, as shown in Fig. 1.

The mathematical model for the interaction of the radiation with the participating medium considering no emission inside the medium, isotropic scattering, and azymuthal symmetry is given by the linear version of the Boltzmann equation [Özisik (1973)]

$$\mu \frac{\partial I(x,\mu)}{\partial x} + \beta I(x,\mu) = \frac{\sigma_s}{2} \int_{-1}^{1} I(x,\mu')d\mu' \quad \text{in } 0 < x < L,\ -1 \le \mu \le 1 \tag{1a}$$

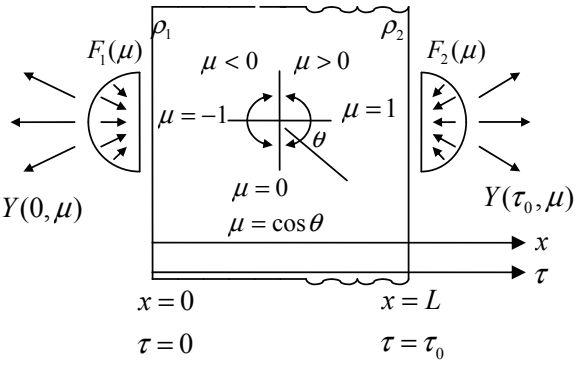

Figure 1: Schematic representation of the one-dimensional participating medium.

$$I(0,\mu) = F_1(\mu) + 2\rho_1 \int_0^1 I(0,-\mu')\mu' d\mu', \quad \mu > 0 \tag{1b}$$

$$I(L,\mu) = F_2(\mu) + 2\rho_2 \int_0^1 I(L,\mu')\mu' d\mu', \quad \mu < 0 \tag{1c}$$

where $I(x,\mu)$ represents the radiation intensity, x is the spatial variable, μ is the cosine of the polar angle θ, i.e. the angle formed by the radiation beam and the positive x axis, $\sigma_s$is the scattering coefficient, ρ_1 and ρ_2 are the diffuse reflectivities at boundaries $x = 0$ and $x = L$, respectively, $F_1(\mu)$ and $F_2(\mu)$ represent the strength of the external sources, and β is the total extinction coefficient defined as

$$\beta = \kappa_a + \sigma_s \tag{2}$$

where κ_a is the absorption coefficient. In Fig. 1, Y represents the radiation that leaves the medium and may be measured using external detectors.

In radiative transfer it is usual to define the optical variable, τ, as

$$d\tau = \beta dx \Rightarrow \tau = \int_0^x \beta dx' \tag{3}$$

Thus, the optical thickness of the medium, τ_0, can be obtained by integrating the whole spatial domain, i.e. from $x = 0$ up to $x = L$ in Eq. (3),

$$\tau_0 = \int_0^L \beta dx' \tag{4a}$$

For a homogeneous medium one obtains

$$\tau_0 = \beta L \tag{4b}$$

Therefore, Eqs. (1a-c) can be reformulated as [Özisik (1973)]

$$\mu \frac{\partial I(\tau,\mu)}{\partial \tau} + I(\tau,\mu) = \frac{\omega}{2} \int_{-1}^{1} I(\tau,\mu')d\mu' \quad \text{in } 0 < \tau < \tau_0,\ -1 \le \mu \le 1 \tag{5a}$$

$$I(0,\mu) = F_1(\mu) + 2\rho_1 \int_0^1 I(0,-\mu')\mu' d\mu', \quad \mu > 0 \tag{5b}$$

$$I(\tau_0,\mu) = F_2(\mu) + 2\rho_2 \int_0^1 I(\tau_0,\mu')\mu' d\mu', \quad \mu < 0 \tag{5c}$$

where ω is the single scattering albedo, which is the ratio between the scattering coefficient and the total extinction coefficient,

$$\omega = \frac{\sigma_s}{\beta} = \frac{\sigma_s}{\kappa_a + \sigma_s} \tag{6}$$

When the geometry, the boundary conditions, and the radiative properties τ_0, ω, ρ_1 and ρ_2 are known, problem (5) may be solved, and the radiation intensity, $I(\tau,\mu)$, can be calculated for the whole spatial and angular domains, i.e. $0 \le \tau \le \tau_0$ and $-1 \le \mu \le 1$. This is the so called direct problem.

In order to solve the direct problem we have used Chandrasekhar's discrete ordinates method [Chandrasekhar (1960)] in which the polar angle domain is discretized, and the integral term on the right hand side of Eq. (5a) is replaced by a gaussian quadrature. We then used a finite-difference approximation for the terms on the left hand side of Eq. (5a), and by performing forward and backward sweeps, from $\tau = 0$ to $\tau = \tau_0$ and from $\tau = \tau_0$ to $\tau = 0$, respectively, $I(\tau,\mu)$ is determined for all spatial and angular nodes of the discretized computational domain. More details can be found in [Pinheiro, Silva Neto and Moura Neto (2002)].

3 Mathematical formulation and solution of the inverse problem

Suppose that the following vector of radiative properties is unknown

$$\overrightarrow{Z} = \{\tau_0, \omega, \rho_1, \rho_2\}^T. \tag{7}$$

Nonetheless experimental data on the radiation that leaves the medium, i.e. Y_i, $i = 1,2,...,N_d$, where N_d is the number of experimental data, are available, acquired with external detectors located at $\tau = 0$ and $\tau = \tau_0$. One may then try to estimate the unknowns using the available experimental data. This is the so called inverse radiative transfer problem.

As schematically represented in Fig. 1, half of the data is acquired at the boundary $\tau = 0$, and half at $\tau = \tau_0$, using, as mentioned before, only external detectors.

As we consider the number of experimental data, N_d, to be larger than the number of unknowns, N_u, i.e. $N_d > N_u$, we formulate the inverse problem implicitly, as an optimization problem, in which we want to minimize the objective function given by

$$Q(\overrightarrow{Z}) = \sum_{i=1}^{N_d} [I_{calc_i}(\overrightarrow{Z}) - Y_i]^2 \tag{8}$$

where I_{calc_i} and Y_i represent the calculated and measured values, respectively, of the intensity of the radiation that leaves the medium at a polar angle θ_i, being $i = 1,2,...,\frac{N_d}{2}$ related to the boundary $\tau = \tau_0$, with $\mu_i = \cos\theta_i > 0$, and $i = \frac{N_d}{2} + 1, \frac{N_d}{2} + 2, ..., N_d$ related to the boundary $\tau = 0$, with $\mu_i = \cos\theta_i < 0$.

For the minimization of the objective function described in Eq. (8), and thus determining the solution of the inverse problem, it has been used both the Luus-Jaakola method and the Particle Collision Algorithm. These optimization methods are described next.

3.1 The Luus-Jaakola method

Random search methods for optimization are based on a random exploration of a domain to find a point that minimizes an objective function. They were originally introduced by Anderson (1953), and then developed by Karnopp (1963) and Matyas (1965), among others.

Random search methods have been widely employed in chemical engineering for continuous optimization as, for example, those proposed by Luus and Jaakola (1973), Gaines and Gaddy (1976), and Salcedo, Gonçalves and Azevedo (1990). The most popular of these techniques is the Luus-Jaakola algorithm (LJ), which has been used not only in chemical engineering [Lee, Rangaiah and Luus (1999); Luus and Hennessy (1999)], but also in control problems [Luus (2001)], in optics [Al-Marzoug and Hodgson (2006)], in electrical engineering [Singh (2005)], and in chromatography [Poplewska, Piatkowski and Antos (2006)], among other applications.

The idea behind the Luus-Jaakola algorithm is very simple: random solutions are selected over a region that is decreased in size as iterations proceed.

Our implementation of LJ is described in Fig. 2. It differs from the original algorithm proposed by Luus and Jaakola (1973) in one point: while, originally, **x*** was replaced by a possible improved solution only after the internal loop was completed, we replace **x*** immediately if a better solution is found, as suggested by Gaines and Gaddy (1976) in their optimization algorithm. This version of the Luus-Jaakola algorithm outperformed the Genetic Algorithm (GA), Simulated Aneealing (SA), the Great Deluge Algorithm (GDA) and the Particle Collition Algorithm (PCA) and performed well compared to the Particle Swarm Optimization (PSO) in a nuclear reactor core design optimization problem [Sacco, Alves Filho and Platt (2008)].

Choose an initial search size $\mathbf{r}^{(0)}$.
Choose a number of external loops n_{out} and a number of internal loops n_{in}.
Choose a contraction coefficient ε.
Generate an initial solution $\mathbf{x}^*$.
For i = 1 to n_{out}
  For j = 1 to n_{in}
    $\mathbf{x}^{(j)} = \mathbf{x}^* + \mathbf{R}^{(j)}\mathbf{r}^{(i-1)}$, where $\mathbf{R}^{(j)}$ is a diagonal matrix of random numbers between -0.5 and 0.5.
    If Fitness ($\mathbf{x}^{(j)}$) < Fitness ($\mathbf{x}^*$)
      $\mathbf{x}^* = \mathbf{x}^{(j)}$
    End If
  End For
  $\mathbf{r}^{(i)} = (1-\varepsilon)\mathbf{r}^{(i-1)}$, where ε is the search size contraction coefficient.
End For

Figure 2: The Luus-Jaakola (LJ) pseudo code.

3.2 The Particle Collision Algorithm

The Particle Collision Algorithm (PCA) [Sacco, Oliveira and Pereira (2006)] is loosely inspired in the physics of the interactions of neutrons in a nuclear reactor [Duderstadt and Hamilton (1976)], mainly scattering, being an incident particle scattered by a target nucleus, and absorption, being the incident particle absorbed by the target nucleus. Thus, a particle that hits a high-fitness "nucleus" would be absorbed, and would explore its neighborhood. On the other hand, a particle that hits a low-fitness region would be scattered to another region. This procedure permits the exploration of the search space and the exploitation of the most promising

areas of the fitness landscape through successive scattering and absorption collision events.

The PCA resembles in its structure that of the Simulated Annealing (SA) [Kirkpatrick, Gellat and Vecchi (1983)], i.e. first an initial configuration is chosen, and then a new configuration is obtained by performing a modification in the previous one. The quality of the two configurations is compared. A decision is then made on whether the new configuration is "acceptable".

If that is the case, it becomes the old configuration for the next step of the iterative procedure. Otherwise, the algorithm proceeds with a new different change of the previous old configuration.

The PCA may also be considered a Metropolis algorithm [Metropolis, Rosenbluth, Rosenbluth, Teller and Teller (1953)], i.e. a trial solution can be accepted with a certain probability even if the new configuration is worse than the old configuration. Such flexibility of the algorithm may avoid the convergence to local minima.

In Fig. 3 is shown the pseudo-code for the PCA in its version for minimization problems. The "stochastic perturbation" mentioned at the beginning of the loop shown in Fig. 3 consists in random variations taken from a uniform distribution in the values of each variable within their ranges prescribed a priori, as shown in Fig. 4.

If the quality or fitness of the new configuration is better than the fitness of the old configuration, then the "particle" is "absorbed", and an exploration of the neighborhood searching for an even better solution takes place. Function "Exploitation ( )" performs this local search, generating a small stochastic perturbation of the solution inside a loop. The "small stochastic perturbation" is similar to the previous stochastic perturbation, but each variable's new value is kept within a small vicinity of the original value, which is here defined in range of $\pm 20\%$, as shown in Fig. 5. Otherwise, if the quality of the new configuration is worse than the one for the old configuration, the "particle" is "scattered". The scattering probability ($p_{scattering}$) is inversely proportional to its quality. A low-fitness particle will have a greater scattering probability. In a process similar to Monte Carlo's "Russian Roulette" [Duderstadt and Martin (1979)], the configuration is "scattered" (replaced by a random configuration) or, following Metropolis, survives, with its neighborhood being further explored ("else" branch of the function).

4 Results and discussion

As real experimental data on the intensity of the exit radiation were not available, we have generated sets of synthetic experimental data. In order to simulate the measured exit intensities,Y_i, containing measurement errors, random errors of normal

```
Generate an initial solution Old_Config
Best Fitness = Fitness (Old_Config)
For n = 0 to # of iterations
        Perturbation( )
        If Fitness(New_Config) > Fitness(Old_Config)
                If Fitness(New_Config) > Best Fitness
                        Best Fitness := Fitness(New_Config)
                End If
                Old_Config := New_Config
                Exploitation ( )
        Else
                Scattering ( )
        End If
End For

Exploitation ( )
        For n = 0 to # of iterations
                Small_Perturbation( )
                If Fitness(New_Config) > Fitness(Old_Config)
                        Old_Config := New_Config
                End If
        End For
return

Scattering ( )
        p_scattering = 1 - Fitness(New_Config) / Best Fitness
        If p_scattering > random (0, 1)
                Old_Config := random solution
        Else
                Exploitation ( );
        End if
return
```

Figure 3: The PCA pseudo code.

```
Perturbation( )
        For i = 0 to (Dimension-1)
        Upper := Superior Limit [i]
        Lower := Inferior Limit [i]
        Rand = Random(0,1)
        New_Config[i] := Old_Config[i] +
                                    +   ((Upper - Old_Config[i])*Rand) –
                                    –   ((Old_Config[i] - Lower)*(1-Rand))
                If (New_Config[i] > Upper)
                        New_Config[i] := SupLim[i];
                Else
                        If (New_Config[i] < Lower)
                                New_Config[i] := InfLim[i];
                        End If
                End If
        End For
End
```

Figure 4: Function "Perturbation" of PCA.

distribution and of standard deviation σ_e are added to the exact intensities computed from the solution of the direct problem. Thus we have

$$Y_i = I_{calc_i}(\overrightarrow{Z}_{exact}) + \sigma_e \cdot r \tag{9}$$

where r is a random number, from a Gaussian distribution, with zero mean and unitary standard deviation.

In order to examine the performance of the methods PCA and LJ for the solution of the inverse radiative transfer problem described in Section 3, several test cases have been studied with and without noise in the synthetic experimental data. In the present work, the three sets of radiative properties shown in Tab. 1 were considered as test cases, and the intensities for the external radiation sources in Eqs. (5b-c) were considered as $F_1 = 1.0$ and $F_2 = 0.0$.

```
Small_Perturbation( )
    For i = 0 to (Dimension-1)
        Upper = Random(1.0, 1.2) * Old_Config[i]
        If (Upper > Superior Limit [i])
            Upper = Superior Limit [i]
        End If
        Lower = Random(0.8, 1.0) * Old_Config[i]
        If (Lower < Inferior Limit [i])
            Lower = Inferior Limit [i]
        End If
        Rand = Random(0,1)
        New_Config[i] = Old_Config[i] +
                    +   ((Upper – Old_Config[i])*Rand) –
                    –   ((Old_Config[i] – Lower)*(1–Rand))
    End For
End
```

Figure 5: Function "Small Perturbation" of PCA.

Table 1: Exact values of the radiative properties

Radiative property	Case 1	Case 2	Case 3
Optical thickness, τ_0	1.0	0.5	2.0
Scattering albedo, ω	0.5	0.1	0.9
Diffuse reflectivity, ρ_1	0.1	0.1	0.5
Diffuse reflectivity, ρ_2	0.9	0.9	0.5

These cases were intentionally chosen for yielding a relatively difficult test for the evaluation of the optimization algorithms. The Cases 1, 2 and 3 were set with $\sigma_e = 0.0005$, 0.0004 and 0.004 respectively. These values lead to errors in the order of, or smaller than, 5.5%.

The PCA was set with $n_{PCA} = 200$ and $n_{\text{exploitation}} = 500$. The LJ was set with

$n_{LJ,out} = 200$, $n_{LJ,in} = 200$ and the contraction coefficient was set as 5%, i.e. $\varepsilon = 0.05$. These parameters were chosen so that the PCA and the LJ present about the same computational effort, evaluating around 40,000 times the objective function. An investigation on the influence of these parameters in the solution of the problem here presented was performed in [Knupp (2008)].

The ranges considered in the PCA and LJ for the search of the unknowns was [0.0,3.0] for τ_0, and [0.0,1.0] for ω, ρ_1 and ρ_2. These are the real physical bounds for the unknowns, except for τ_0 which may have a higher value than the upper bound considered. Nonetheless, it must be stressed that $\tau_0 = 3.0$ is already a high value if one wants to consider the information on the transmitted radiation for the inverse problem solution. For each case (1-3 in Tab. 1), 10 runs were performed for each method (PCA and LJ). All runs were performed on a PC with the processor AMD Turion™ 63 X2 Mobile (1.60 GHz with 1.37 GB of RAM) and took around 2h40min with both methods PCA and LJ. In Tabs. 2-4 are presented the average, μ_Z, the standard deviation, σ_Z, the best and the worst estimates, $\vec{Z}_{best}$ and $\vec{Z}_{worst}$ respectively, for each radiative property obtained with the PCA and the LJ. Here the worst estimates obtained for each method correspond to the run, among the 10 runs performed for each method, for which the objective function is the highest at the end of the run, and the best estimates correspond to the run for which the value of the objective function is the lowest.

Table 2: Results obtained with the PCA and the LJ for Case 1. $\sigma_e = 0.0005$ (5.5%).

		τ_0	ω	ρ_1	ρ_2	$Q\left(\vec{Z}\right)$, Eq. (8)
$\vec{Z}_{exact}$		1.0	0.5	0.1	0.9	-
PCA	$\vec{Z}_{worst}$	1.003	0.515	0.145	0.901	3.80E-05
	$\vec{Z}_{best}$	1.004	0.507	0.116	0.902	6.44E-06
	μ_Z	1.002	0.498	0.092	0.899	
	σ_Z	0.006	0.010	0.032	0.002	
	$\frac{\sigma_Z}{\mu_Z} \times 100\%$	0.6%	1.9%	34.6%	0.3%	
LJ	$\vec{Z}_{worst}$	1.002	0.494	0.081	0.899	5.69E-06
	$\vec{Z}_{best}$	1.001	0.502	0.104	0.900	1.90E-06
	μ_Z	0.999	0.502	0.106	0.900	
	σ_Z	0.002	0.004	0.015	0.001	
	$\frac{\sigma_Z}{\mu_Z} \times 100\%$	0.2%	0.8%	13.8%	0.1%	

Even though good estimates have been obtained with both methods (PCA and LJ), as it can be observed in Tabs. 2-4, the standard deviations of the estimates obtained for ρ_1 were relatively high in Cases 1 and 2, what indicates that even though the

Table 3: Results with the PCA and the LJ for Case 2. $\sigma_e = 0.0004$ (5.5%).

		τ_0	ω	ρ_1	ρ_2	$Q\left(\vec{Z}\right)$, Eq. (8)
$\vec{Z}_{exact}$		0.5	0.1	0.1	0.9	-
PCA	$\vec{Z}_{worst}$	0.470	0.124	0.140	0.906	2.22E-04
	$\vec{Z}_{best}$	0.499	0.115	0.124	0.899	4.18E-05
	μ_Z	0.485	0.110	0.113	0.904	
	σ_Z	0.029	0.010	0.077	0.006	
	$\frac{\sigma_Z}{\mu_Z} \times 100\%$	6.0%	9.4%	47.7%	0.7%	
LJ	$\vec{Z}_{worst}$	0.504	0.102	0.08	0.9	1.57E-05
	$\vec{Z}_{best}$	0.502	0.102	0.098	0.9	5.97E-06
	μ_Z	0.502	0.101	0.105	0.901	
	σ_Z	0.002	0.002	0.021	0.002	
	$\frac{\sigma_Z}{\mu_Z} \times 100\%$	0.5%	1.7%	20.3%	0.2%	

Table 4: Results obtained with the PCA and the LJ for Case 3. $\sigma_e = 0.004$ (5%).

		τ_0	ω	ρ_1	ρ_2	$Q\left(\vec{Z}\right)$, Eq. (8)
$\vec{Z}_{exact}$		2.0	0.9	0.5	0.5	-
PCA	$\vec{Z}_{worst}$	2.18	0.92	0.549	0.44	1.79E-03
	$\vec{Z}_{best}$	1.952	0.897	0.495	0.511	2.97E-04
	μ_Z	2.114	0.907	0.517	0.488	
	σ_Z	0.159	0.012	0.032	0.029	
	$\frac{\sigma_Z}{\mu_Z} \times 100\%$	7.5%	1.4%	6.2%	6.0%	
LJ	$\vec{Z}_{worst}$	1.731	0.883	0.46	0.527	2.13E-04
	$\vec{Z}_{best}$	2.127	0.905	0.51	0.477	7.58E-05
	μ_Z	1.889	0.893	0.483	0.509	
	σ_Z	0.142	0.008	0.017	0.022	
	$\frac{\sigma_Z}{\mu_Z} \times 100\%$	7.5%	0.9%	3.5%	4.2%	

average may be near the exact value, the estimates are not accurate. This is in fact the main difficulty associated with Cases 1 and 2, i.e., the low values of ρ_1 combined with the external illumination given by $F_1 = 1.0$ and $F_2 = 0.0$, in Eq. (1a-c). The effect of ρ_1 will be sensed by the external detectors only after the radiation goes into the medium at $\tau = 0$, is reflected at $\tau = \tau_0$ and is then both transmitted and reflected at $\tau = 0$. The low sensitivity of the exit radiation intensities to this particular unknown is confirmed by a sensitivity analysis [Knupp, Silva Neto and

Sacco (2009)].

In Case 3, the standard deviations of all unknowns are higher than in Cases 1 and 2. The main difficulty in this case is the high value of the optical thickness, τ_0. As mentioned before, high values for this property bring difficulty when one wants to consider the information on the transmitted radiation for the inverse problem solution.

It is also important to observe that the LJ was able to obtain estimates with lower values of the objective function and lower standard deviations for all cases.

Table 5: Results obtained with the PCA-LJ for Case 1. $\sigma_e = 0.0005$ (5.5%).

		τ_0	ω	ρ_1	ρ_2	$Q\left(\vec{Z}\right)$, Eq. (8)
$\vec{Z}_{exact}$		1.0	0.5	0.1	0.9	-
PCA-LJ	$\vec{Z}_{worst,PCA}$	0.934	0.650	0.505	0.937	2.86E-04
	$\vec{Z}_{worst}$	1.004	0.510	0.130	0.901	1.79E-05
	$\vec{Z}_{best,PCA}$	0.992	0.566	0.294	0.914	7.54E-05
	$\vec{Z}_{best}$	1.004	0.500	0.099	0.898	6.02E-06
	μ_Z	1.002	0.505	0.115	0.901	
	σ_Z	0.005	0.004	0.014	0.001	
	$\frac{\sigma_Z}{\mu_Z} \times 100\%$	0.5%	0.8%	12.6%	0.2%	

Table 6: Results obtained with the PCA-LJ for Case 2. $\sigma_e = 0.0004$ (5.5%).

		τ_0	ω	ρ_1	ρ_2	$Q\left(\vec{Z}\right)$, Eq. (8)
$\vec{Z}_{exact}$		0.5	0.1	0.1	0.9	-
PCA-LJ	$\vec{Z}_{worst,PCA}*$	1.642	0.982	0.958	0.991	5.83E-02
	$\vec{Z}_{worst}*$	1.581	0.998	0.972	0.993	5.51E-02
	$\vec{Z}_{best,PCA}$	0.486	0.202	0.304	0.916	2.63E-03 *
	$\vec{Z}_{best}$	0.501	0.100	0.096	0.900	8.32E-07
	μ_Z	0.501	0.097	0.094	0.899	
	σ_Z	0.003	0.002	0.019	0.002	
	$\frac{\sigma_Z}{\mu_Z} \times 100\%$	0.6%	1.7%	20.9%	0.2%	

* This run was the only one that did not converge and it was not included in the calculation of the average.

In Figs. 6-8 are presented the estimates obtained with both PCA and LJ methods for each case (1-3 in Tab. 1). It is also shown the exact values of the properties, the

Table 7: Results obtained with the PCA-LJ for Case 3. $\sigma_e = 0.004$ (5.5%).

		τ_0	ω	ρ_1	ρ_2	$Q\left(\vec{Z}\right)$, Eq. (8)
$\vec{Z}_{exact}$		2.0	0.9	0.5	0.5	-
PCA-LJ	$\vec{Z}_{worst,PCA}$	1.484	0.864	0.417	0.556	3.90E-04
	$\vec{Z}_{worst}$	1.716	0.884	0.464	0.538	2.75E-04
	$\vec{Z}_{best,PCA}$	1.875	0.877	0.410	0.438	2.01E-03
	$\vec{Z}_{best}$	1.951	0.896	0.486	0.504	8.79E-05
	μ_Z	1.954	0.896	0.489	0.503	
	σ_Z	0.201	0.015	0.002	0.018	
	$\frac{\sigma_Z}{\mu_Z} \times 100\%$	10.3%	1.7%	4.1%	3.6%	

Table 8: Relative standard deviations of the estimates obtained with PCA, LJ and PCA-LJ.

Test Case	Method	$\frac{\sigma_{\tau_0}}{\mu_{\tau_0}} \times 100\%$	$\frac{\sigma_\omega}{\mu_\omega} \times 100\%$	$\frac{\sigma_{\rho_1}}{\mu_{\rho_1}} \times 100\%$	$\frac{\sigma_{\rho_2}}{\mu_{\rho_2}} \times 100\%$
1	PCA	0.6%	1.9%	34.6%	0.3%
	LJ	0.2%	0.8%	13.8%	0.1%
	PCA-LJ	0.5%	0.8%	12.6%	0.2%
2	PCA	6.0%	9.4%	47.7%	0.7%
	LJ	0.5%	1.7%	20.3%	0.2%
	PCA-LJ	0.6%	1.7%	20.9%	0.2%
3	PCA	7.5%	1.4%	6.2%	6.0%
	LJ	7.5%	0.9%	3.5%	4.2%
	PCA-LJ	10.3%	1.7%	4.1%	3.6%

average of the estimates and the confidence bounds for the average. As the sample size is relatively small (10 runs), the confidence bounds have been calculated based on the Student's T distribution as

$$\left(\mu_Z - t_{(n-1),(1-C)} \times \frac{\sigma_Z}{\sqrt{n}},\ \mu_Z + t_{(n-1),(1-C)} \times \frac{\sigma_Z}{\sqrt{n}}\right) \tag{10}$$

where $t_{(n-1),(1-C)}$ is the critical value for the Student's T distribution with n data points, i.e., $n-1$ degrees of freedom, and C% confidence. For all cases presented in this work, we have 10 runs, i.e. $n = 10$. Considering 99% confidence, $t_{(n-1),(1-C)} = t_{(9),(0.01)} = 3.250$.

As expected, it can be observed in Figs. 6-8 that the confidence bounds for ρ_1 are relatively wide in Cases 1 and 2, and the confidence bounds for all unknowns are wider in Case 3.

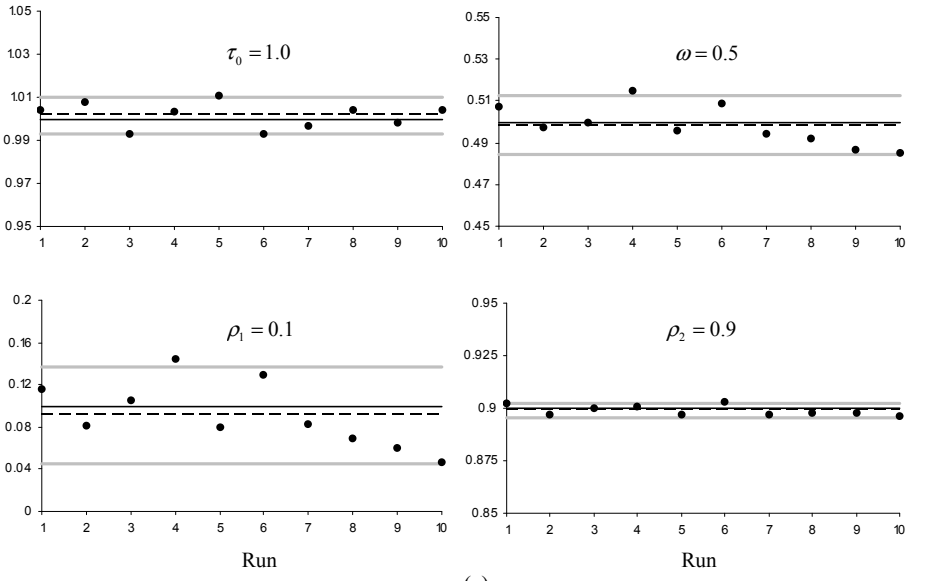

(a)

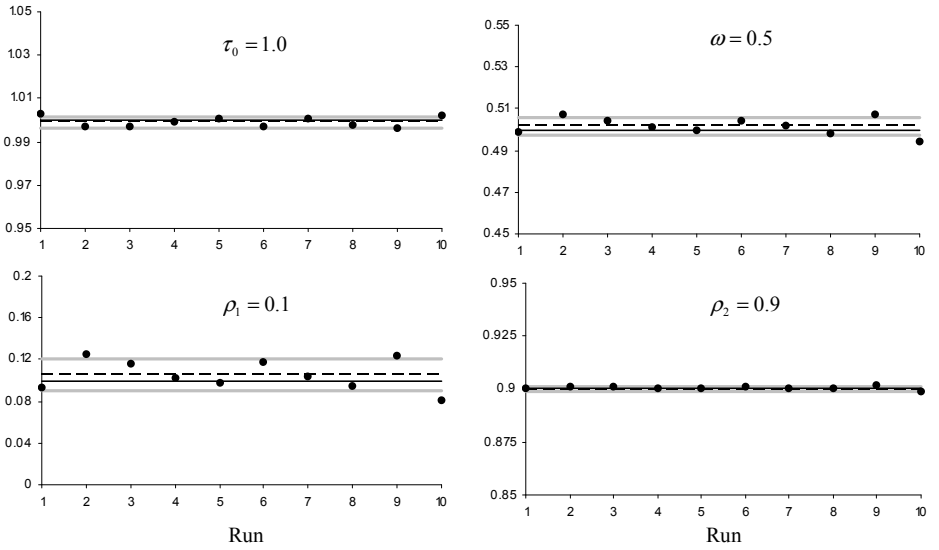

(b)

Figure 6: Results obtained with both PCA (a) and LJ (b) methods. Case 1. $\sigma_e =$ 0.0005 (5.5%). — exact values; - - - average; ▬ confidence bounds; • estimates.

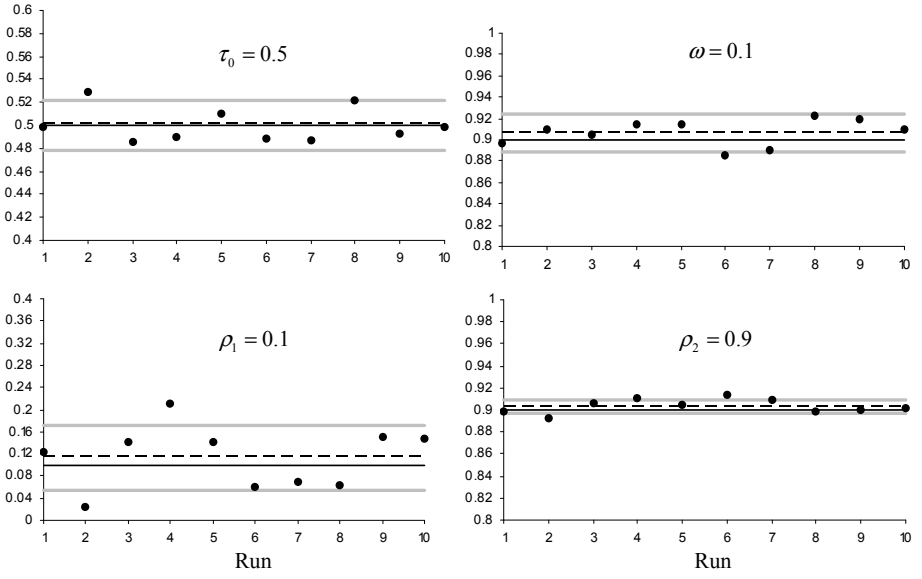

(a)

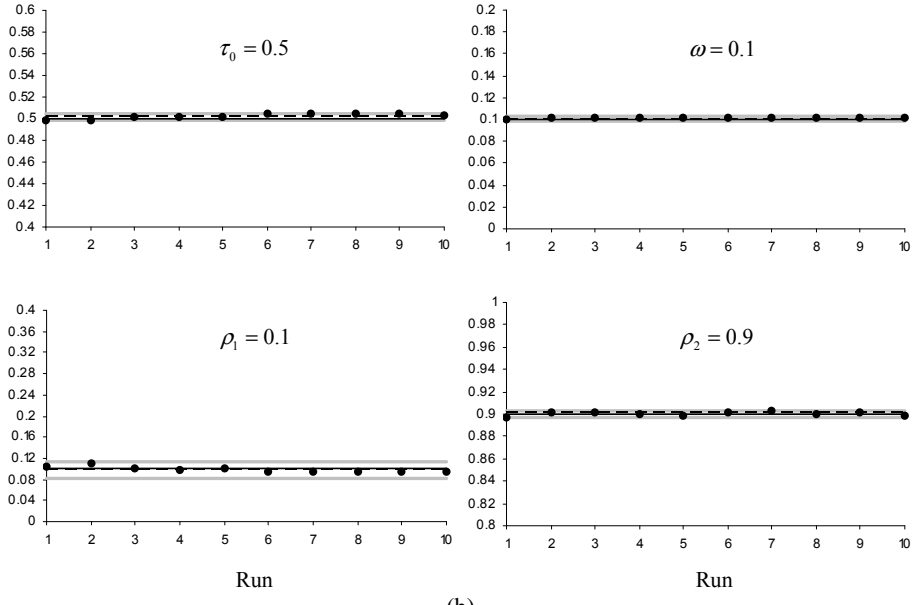

(b)

Figure 7: Results obtained with both PCA (a) and LJ (b) methods. Case 2. $\sigma_e = 0.0005$ (5.5%). — exact values; - - - average; ▬ confidence bounds; • estimates.

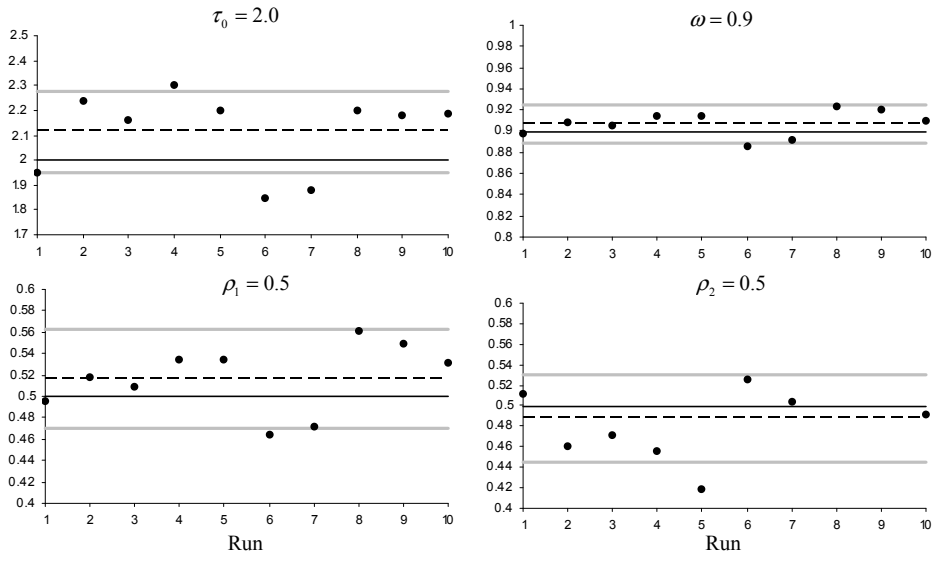

(a)

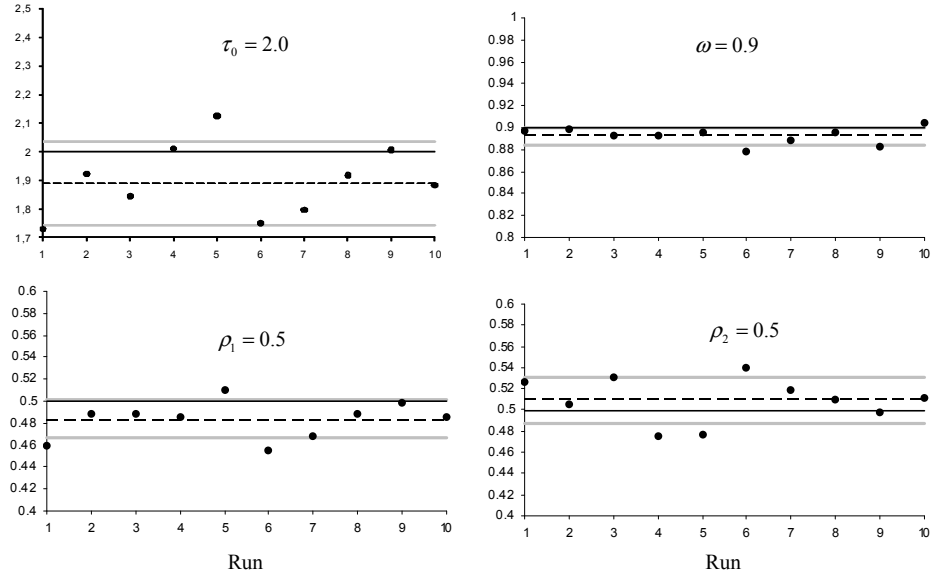

(b)

Figure 8: Results obtained with both PCA (a) and LJ (b) methods. Case 3. $\sigma_e =$ 0.0005 (5.5%). — exact values; - - - average; ▬ confidence bounds; • estimates.

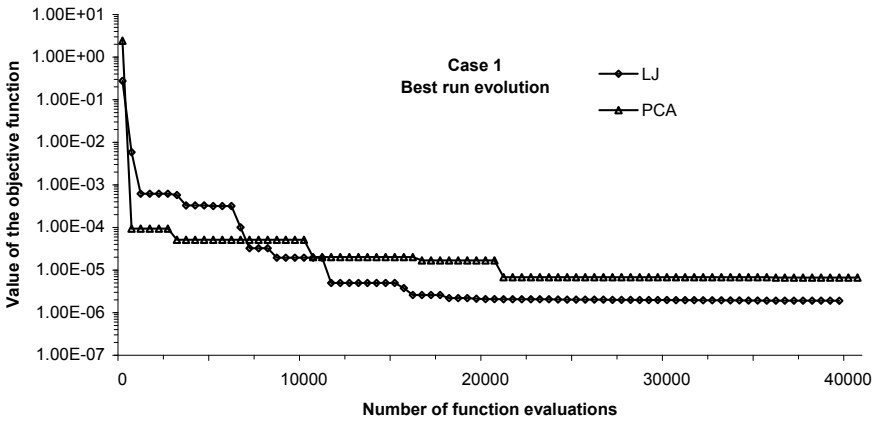

Figure 9: Evolution of the objective function. Case 1.

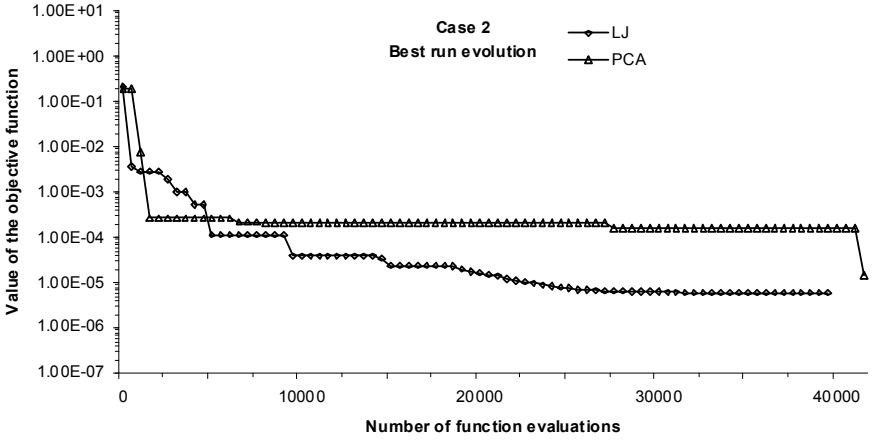

Figure 10: Evolution of the objective function. Case 2.

It is also important to observe that the confidence bounds are narrower with the LJ than with the PCA, for all unknowns, in all cases presented here. This is related with the fact that the LJ was able to obtain estimates with lower values of the objective function, as it can be observed in Tabs. 2-4.

In Figs. 9-11 are shown the evolutions of the objective function for the best runs obtained with both the PCA and the LJ.

It is interesting to observe that even though the LJ reaches a lower value of the

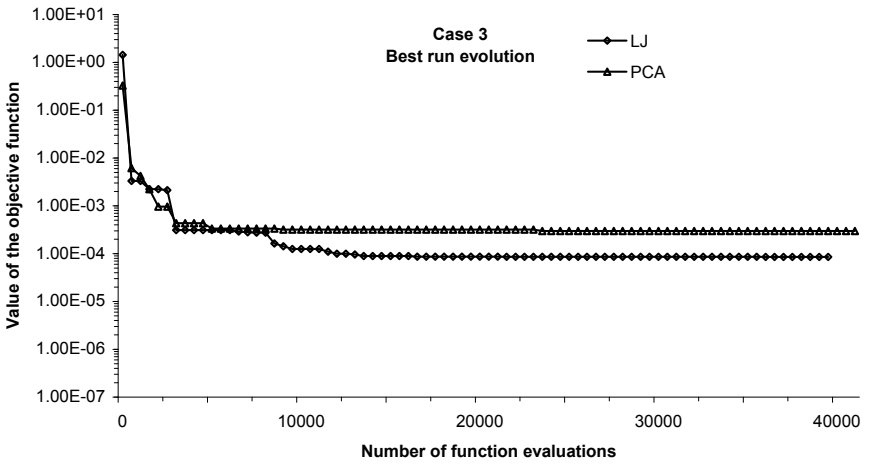

Figure 11: Evolution of the objective function. Case 3.

objective function, the PCA performs better at the beginning of the search. As it can be seen in Figs. 9-11, the PCA performed better until around 7,500 function evaluations in Case 1 and until around 5,000 function evaluations in Case 2. In Case 3, the methods performed competitively until around 8,000 iterations.

Such fact may explain the good results obtained by the PCA in a hybrid strategy, where the stochastic method is used for a few number of function evaluations, just to find regions of local optima to be further exploited by a gradient based method as investigated by [Knupp, Silva Neto and Sacco (2007)].

With that in mind, it was proposed the use of the PCA set with $n_{PCA} = 3$ and $n_{\text{exploitation}} = 500$, in order to generate an initial guess for the LJ set with $n_{LJ,out} = 142$, $n_{LJ,in} = 200$, and the search space beginning as if 58 iterations had already been performed. With such configuration the LJ performs 11,600 less evaluations of the cost function. With this hybrid approach, named PCA-LJ, each run took around 1h55min (26% faster than the canonical LJ with $n_{LJ,out} = 200$ and $n_{LJ,in} = 200$).

The results of 10 runs are presented in Tabs. 5-7 for Cases 1, 2 and 3, respectively. $\vec{Z}_{worst,PCA}$ and $\vec{Z}_{best,PCA}$ represents the initial guess of the worst and the best estimate, respectively.

As it can be observed in Tabs. 5-7, with exception of one run that did not converge for Case 2, the results obtained by the PCA-LJ were as good as those obtained by the LJ, with less computational effort (26% faster). In Tab. 8 are presented the

relative standard deviations of the estimates obtained with each one of the three methods presented in this work: PCA, LJ and PCA-LJ. Regarding the worst run for Case 2, it is important to stress that among the 10 runs performed, that was the only one that did not converge and it was not included in the calculation of the average.

5 Conclusion

From the results presented in the previous section one concludes that .both the PCA and the LJ provides good solutions for the inverse problem of radiative transfer properties estimation. Joining the better performance of the PCA in the beginning of the search with the better accuracy provided by LJ it was possible to implement the hybrid version PCA-LJ, which performed even better. As further development of this approach, it may be considered in future works the use of a hybrid version of the PCA with the Nelder-Mead Simplex, which was successfully applied in nuclear reactors core design [Sacco, Alves Filho, Henderson and Oliveira (2008)].

Acknowledgement: The authors acknowledge the financial support provided by CNPq, Conselho Nacional de Desenvolvimento Científico e Tecnológico, FAPERJ (Fundação Carlos Chagas Filho de Amparo à Pesquisa do Estado do Rio de Janeiro) and FAPESPA (Fundação de Amparo à Pesquisa do Estado doPará).

References

Al-Marzoug, S. M.; Hodgson, R. J. W. (2006): Optimization of Platinum-Carbon Multilayer Mirrors for Hard X-ray Optics. *Optics Communications*, vol. 268, no. 1, pp. 84–89.

An, W.; Ruan, L. M.; Qi, H. (2007): Inverse Radiation Problem in One-Dimensional Slab by Time-Resolved Reflected and Transmitted Signals. *Journal of Quantitative Spectroscopy & Radiative Transfer*, vol. 107, pp. 47–60.

Anderson, R. (1953): Recent Advances in Finding Best Operating Conditions. *J. Amer. Statist. Assoc.*, vol. 48, pp. 789–798.

Buehler, S. A.; Eriksson, P.; Kuhn, T.; von Engeln, A.; Verdes, C. (2005): ARTS, the Atmospheric Radiative Transfer Simulator. *Journal of Quantitative Spectroscopy & Radiative Transfer*, vol. 91, no. 1, pp. 65–93.

Carita Monteiro, R. F.; Roberty, N. C.; Silva Neto, A. J. (2004): Reconstruction of a Combination of the Absorption and Scattering Coefficients with a Discrete Ordinates Method Consistent with the Source-Detector System. *Inverse Problems in Engineering*, vol. 12, no. 1, pp. 81–101.

Chalhoub, E. S.; Campos Velho, H. F. (2001): Simultaneous Estimation of Ra-

diation Phase Function and Albedo in Natural Waters. *Journal of Quantitative Spectroscopy & Radiative Transfer*, vol. 69, pp. 137–149.

Chandrasekhar, S. (1960): *Radiative Transfer*. Dover Publications, inc., New York, USA.

Duderstadt, J. J.; Martin, W. R. (1979): *Transport Theory*. John Wiley & Sons, New York, USA.

Duderstadt, J. J.; Hamilton, L. J. (1976): *Nuclear Reactor Analysis*. John Wiley & Sons, New York, USA.

Gaines, L. D.; Gaddy, J. L. (1976): Process Optimization by Flow Sheet Simulation. *Ind Eng Chem. Process Des Dev*, vol. 15, no. 1, pp. 206–211.

Goldberg, D. E. (1989): *Genetic Algorithms in Search, Optimization & Machine Learning*. Addison-Wesley, Reading, MA, USA.

Hespel, L.; Mainguy, S.; Greffet, J. J. (2003): Radiative Properties of Scattering and Absorbing Dense Media: Theory and Experimental Study. *Journal of Quantitative Spectroscopy & Radiative Transfer*, vol. 77, pp. 193–210.

Hillier, J. K. (1997): Shadow-hiding Opposition Surge for a Two-Layer Surface. *Icarus*, vol. 128, no. 1, pp. 15–27.

Karnopp, D. C. (1963): Random Search Techniques for Optimization Problems. *Automatica*, vol. 1, pp. 111–121.

Kim, H. K.; Charette, A. (2007): A Sensitivity Function – Based Conjugate Gradient Method for Optical Tomography with the Frequency Domain Equation of Radiative Transfer. *Journal of Quantitative Spectroscopy & Radiative Transfer*, vol. 104, pp. 24–39.

Kirkpatrick, S.; Gellat Jr., C. D.; Vecchi, M. P. (1983): Optimizing by Simulated Annealing. *Science*, vol. 220, pp. 671–680.

Knupp, D. C.; Silva Neto, A. J.; Sacco, W. F. (2009): Radiative Properties Estimation with the Particle Collision Algorithm based on a Sensitivity Analysis. *High Temperatures High Pressures*, vol. 38, no. 2, pp. 137-151.

Knupp, D. C.; Silva Neto, A. J.; Sacco, W. F. (2007): Estimation of Radiative Properties with the Particle Collision Algorithm. Proc. Inverse Problems, Design and Optimization Symposium 2007, Miami, Florida, USA.

Knupp, D. C. (2008): *Implementation of Stochastic and Deterministic Methods for Radiative Properties Estimation*. Mechanical Engineering Degree Project, Rio de Janeiro State University, UERJ, Nova Friburgo, Brazil. In Portuguese.

Lee, Y. P.; Rangaiah, G. P.; Luus, R. (1999): Phase and Chemical Equilibrium Calculations by Direct Search Optimization. *Computers and Chemical Engineer-*

ing, vol. 23, pp. 1183–1191.

Liao, B.; Luus, R. (2005): Comparison of the Luus-Jaakola Optimization Procedure and the Genetic Algorithm. *Engineering Optimization*, vol. 37, no. 4, pp. 381–396.

Luus, R. (2001): Use of Luus-Jaakola Optimization Procedure for Singular Optimal Control Problems. *Nonlinear Analysis*, vol. 47, pp. 5647–5658.

Luus, R.; Hennessy, D. (1999): Optimization of Fed-Batch Reactors by the Luus-Jaakola Optimization Procedure. *Ind. Eng. Chem. Res.*, vol. 38, pp. 1948–1955.

Luus, R.; Jaakola, T. H. I. (1973): Optimization by Direct Search and Systematic Reduction of the Size of Search Region. *AIChE Journal*, vol. 19, no. 4, pp. 760–766.

Matyas, J. (1965): Random optimization. *Automation and Remote Control*, vol. 26, pp. 246–253.

Metropolis, N.; Rosenbluth, A. W.; Rosenbluth, M. N.; Teller, H. A.; Teller, E. (1953): Equation of State Calculation by Fast Computing Machines. *Journal of Chemical Physics*, vol. 21, pp. 1087–1092.

Morishima, R.; Salo, H.; Ohtsuki, K. (2009): A Multilayer Model for Thermal Infrared Emission of Saturn's rings: Basic Formulation and Implications for Earth-Based Observations. *Icarus*, vol. 201, no. 2, pp. 634–654.

Mossi, A. C.; Vielmo, H. A.; França, F. H. R.; Howell, J. R. (2008): Inverse Design Involving Combined Radiative and Turbulent Convective Heat Transfer. *International Journal of Heat and Mass Transfer*, vol. 51, no. 11-12, pp. 3217–3226.

Nenarokomov, A.; Titov, D. (2005): Optimal Experiment Design to Estimate the Radiative Properties of Materials. *Journal of Quantitative Spectroscopy & Radiative Transfer*, vol. 93, pp. 313–323.

Özisik, M. N. (1973): *Radiative Transfer and Interactions with Conduction and Convection*. John Wiley, New York, USA.

Pinheiro, R. P. F.; Silva Neto, A. J.; Moura Neto, F. D. (2002): Operator Splitting Techniques for Radiative Transfer in a Participating Medium. Proc. 5th World Congress on Computational Mechanics, Vienna, Austria.

Poplewska, I.; Piatkowski, W.; Antos, D. (2006): Effect of Temperature on Competitive Adsorption of the Solute and the Organic Solvent in Reversed-Phase Liquid Chromatography. *Journal of Chromatography A*, vol. 1103, pp. 284–295.

Ranjbar A. A.; Ezzati, M.; Famouri, M. (2009): Optimization of Experimental Design for an Inverse Estimation of the Metal-mold Heat Transfer Coefficient in the Solidification of Sn–10% Pb. *Journal of Materials Processing Technology,* vol.

209, no. 15-16, pp. 5611–5617.

Sacco, W. F.; Oliveira, C. R. E.; Pereira, C. M. N. A. (2006): Two Stochastic Optimization Algorithms Applied to Nuclear Reactor Core Design. *Progress in Nuclear Energy*, vol. 48, no. 6, pp. 525–539.

Sacco, W. F.; Lapa, C. M. F.; Pereira, C. M. N. A.; Alves Filho, H. (2008): A Metropolis Algorithm Applied to a Nuclear Power Plant Auxiliary Feedwater System Surveillance Tests Policy Optimization. *Progress in Nuclear Energy*, vol. 50, no. 1, pp. 15-21.

Sacco, W. F.; Alves Filho, H.; Platt, G. M. (2008): The Luus-Jaakola Algorithm Applied to a Nuclear Reactor Core Design Optimization. *International Journal of Nuclear Energy Science and Technology*. vol. 4, pp. 1-10.

Sacco, W. F.; Alves Filho, H.; Henderson, N.; Oliveira, C. R. (2008): A Metropolis Algorithm Combined with the Nelder-Mead Simplex Applied to Nuclear Reactor Core Design. *Annals of Nuclear Energy*. vol. 35, pp. 861-867.

Salcedo, R. L.; Gonçalves, M. J.; Azevedo, S. F. (1990): An Improved Random Search Algorithm for Non-Linear Optimization. *Computers and Chemical Engineering*, vol. 14, no. 10, pp. 1111–1126.

Silva Neto, A. J. (2002): Explicit and Implicit Formulations for Inverse Radiative Transfer Problems. Proc. 5th World Congress on Computational Mechanics, Mini-Symposium MS 125 – Computational Treatment of Inverse Problems in Mechanics, Vienna, Austria.

Silva Neto, A. J.; Roberty, N. C.; Pinheiro, R. P. F.; Alvarez Acevedo, N. I. (2007): Inverse Problems Explicit and Implicit Formulations with Applications in Engineering, Biophysics and Biotechnology. *Inverse Problems in Science and Engineering*, vol. 15, no. 4, pp. 373–411.

Singh, V. (2005): Obtaining Routh-Padé Approximants Using the Luus-Jaakola Algorithm. *IEE Proc.-Control Theory Appl.*, vol. 152, no. 2, pp. 129–132.

Sladek, J.; Sladek, V.; Wen, P. H.; Hon, Y. C. (2009): The Inverse Problem of Determining Heat Transfer Coefficients by the Meshless Local Petrov-Galerkin Method. *CMES: Computer Modeling in Engineering & Sciences*, vol. 48, no. 2, pp. 191-218.

Toomey, M.; Roberts, D.; Nelson, B. (2009): The Influence of Epiphylls on Remote Sensing of Humid Forests. *Remote Sensing of Environment*, In Press.

Tsukada, T.; Kobayashi, M.; Jing, C. J.; Imaishi, N. (2005): Numerical Simulation of CZ Crystal Growth of Oxide. *CMES: Computer Modeling in Engineering & Sciences*, vol. 1, no. 1, pp. 45–62.

Wei, D.; Liu, Y.; Xiang, Z. (2009): A Numerical Method for Estimating the Max-

imal Temperature Gradients Reached in Fire-Damaged Concrete Structures Based on the Parameter Identification. *CMES: Computer Modeling in Engineering & Sciences*, vol. 46, no. 1, pp. 77-106.

Weng, Q. (2009): Thermal Infrared Remote Sensing for Urban Climate and Environmental Studies: Methods, Applications, and Trends. *ISPRS Journal of Photogrammetry and Remote Sensing*, In Press.

Yeih, W.; Liu, C.-S. (2009): A Three-Point BVP of Time-Dependent Inverse Heat Source Problems and Solving by a TSLGSM. *CMES: Computer Modeling in Engineering & Sciences*, vol. 46, no. 2, pp. 107-127.

Zhou, J.; Chen, J. K.; Zhang, Y. (2007): Theoretical Analysis of Thermal Damage in Biological Tissues Caused by Laser Irradiation. *CMES: Computer Modeling in Engineering & Sciences*, vol. 4, no. 1, pp. 27–39.